SOME DYNAMIC PROBLEMS OF ROTATING WINDMILL SYSTEMS*

John Dugundji
Massachusetts Institute of Technology

SUMMARY

The basic whirl stability of a rotating windmill on a flexible tower is reviewed. Effects of unbalance, gravity force, gyroscopic moments, and aerodynamics are discussed. Some experimental results on a small model windmill are given.

INTRODUCTION

There has been a renewed interest in the use of large windmills for generating power. Such large, rotating structures mounted on tall flexible towers may give rise to significant vibration and fatigue problems. A good deal of the experience and knowledge gained during the last few years in connection with helicopter rotors and tilt-wing proprotors can be applied to such large windmill systems. However, there are unique features of windmills and their operating environment that will have to be explored individually.

A basic description of general rotating machinery problems can be found in Den Hartog's book, (ref. 1). Loewy (ref. 2) presents a good review of rotary wing dynamic and aeroelastic problems. More recently, a NASA special publication (ref. 3) gives a good sampling of current problems dealing with rotor dynamics. References 4, 5, 6 are typical of recent investigations of problems of large windmill systems. The present article will first review some dynamic problems of a rotating windmill on a flexible tower, then present some preliminary experimental results on a small windmill model.

REVIEW OF THEORY

Figure 1 shows the model used for representing a windmill rotor mounted on a flexible tower. There is an absolute axis system x, y, z fixed in space, and also an axis system x_s, y_s, z_s along the windmill shaft and having x_s lie in the vertical plane (plane of xz). The i^{th} blade rotates about the axis z_s with a constant speed Ω, and can lag an angle ϕ_i in $x_s y_s$ plane and flap an angle β_i perpendicular to $x_s y_s$ plane. Any point, ξ, on the blade can be expressed relative to the shaft axes x_s, y_s, z_s as

*The author would like to acknowledge the support of National Science Foundation Grant AER75-00826.

$$
\begin{aligned}
x_s &= e \cos \psi_i + \xi \cos (\psi_i + \phi_i) \cos \beta_i \\
y_s &= e \sin \psi_i + \xi \sin (\psi_i + \phi_i) \cos \beta_i \\
z_s &= \xi \sin \beta_i
\end{aligned}
\tag{1}
$$

In the above, ψ_i represents the angular position of the i^{th} blade and e is the hinge off-set. The origin of the shaft axis is assumed to translate fore-and-aft a distance q_F and laterally a distance q_L. Associated with these deflections are an angular rotation $\theta_F q_F$ about the y_s axis, another possible rotation $\theta_L q_L$ about the x_s axis, and a vertical deflection $h_v q_F$ in the x direction. The coefficients θ_F, θ_L, h_v can be obtained from the vibration modes of the tower (often, $h_v \approx -h_F$). The shaft axes can be located relative to the fixed axes by performing a rigid body rotation about the y_s axis and about the x_s axis respectively. This gives the relation

$$
\begin{Bmatrix} x \\ y \\ z \end{Bmatrix} = \begin{bmatrix} \cos \theta_F q_F & \sin \theta_F q_F \sin \theta_L q_L & -\sin \theta_F q_F \cos \theta_L q_L \\ & \cos \theta_L q_L & \sin \theta_L q_L \\ \sin \theta_F q_F & -\cos \theta_F q_F \sin \theta_L q_L & \cos \theta_F q_F \cos \theta_L q_L \end{bmatrix} \begin{Bmatrix} x_s \\ y_s \\ z_s \end{Bmatrix}
\tag{2}
$$

Using the small angle approximation, $\sin \theta_F q_F \approx \theta_F q_F$, $\cos \theta_F q_F \approx 1 - \theta_F^2 q_F^2/2$ etc. in equation (2) and combining with equation (1) and the appropriate deflections gives,

$$
\begin{aligned}
x &= h_v q_F + (1 - \theta_F^2 q_F^2/2) x_s + \theta_F q_F \, \theta_L q_L \, y_s - \theta_F q_F \, z_s \\
y &= q_L + (1 - \theta_L^2 q_L^2/2) y_s + \theta_L q_L \, z_s \\
z &= q_F + \theta_F q_F \, x_s - \theta_L q_L \, y_s + (1 - \theta_F^2 q_F^2/2 - \theta_L^2 q_L^2/2) \, z_s
\end{aligned}
\tag{3}
$$

where x_s, y_s, z_s are given by equation (1). The velocity components $\dot{x}$, $\dot{y}$, $\dot{z}$ are obtained from equations (3) by differentiation with respect to time t. Then, by forming the kinetic energy of the blades and tower, and placing into Lagrange's equations, one can obtain the equations of motion of the windmill system. To simplify the lengthy algebra involved, it was assumed the hinge offset e = 0, and only those terms leading to linear terms in the final equations of motion were retained. The following standard mass integrals were defined for the i^{th} blade,

$$
M_i = \int dm, \qquad S_i = \int \xi \, dm, \qquad I_i = \int \xi^2 \, dm
\tag{4}
$$

In the development, a two-bladed rotor was assumed with slightly unequal masses, such that $M_1 = M_\beta + M_u/2$ and $M_2 = M_\beta - M_u/2$ where M_β was the average mass and M_u the unbalance in mass of the blades. Similar definitions were made for the average and unbalance in moment S_β and S_u, and in moment of inertia I_β and I_u. The vertical gravity loads were put in by writing the incremental work as,

$$\delta W = \int [f_x \delta x + f_y \delta y + f_z \delta y] d\xi = \Sigma Q_n \delta q_n \tag{5}$$

where $f_x = -mg$, $f_y = f_z = 0$, δq_n represents δq_F, δq_L, $\delta\beta_i, \delta\phi_i$ respectively, and δx, δy, δz are found by differentiating equation (3). A similar procedure could be used for obtaining the aerodynamic forces acting on the blade. However there, it is convenient to relate the air forces perpendicular and parallel to the blade axis ξ.

The final, linear equations of motion in terms of the six coordinates q_F, q_L, β_1, β_2, ϕ_1, ϕ_2 are,

$$\begin{aligned}
&[M_{TF} + 2M_\beta(1 + h_v^2) + 2\theta_F S_u \cos\psi_1 + \theta_F^2 I_\beta(1 + \cos 2\psi_1)]\ddot{q}_F - \theta_F[S_u \sin\psi_1 \\
&+ \theta_F I_\beta \sin 2\psi_1]2\Omega\dot{q}_F - \theta_F S_u \cos\psi_1 \Omega^2 q_F + c_F\dot{q}_F + k_F q_F - \theta_L[S_u \sin\psi_1 \\
&+ \theta_F I_\beta \sin 2\psi_1]\ddot{q}_L - \theta_L[S_u \cos\psi_1 + \theta_F I_\beta(1 + \cos 2\psi_1)]2\Omega\dot{q}_L + \theta_L S_u \sin\psi_1 \Omega^2 q_L \\
&+ \sum^i (S_i + \theta_F I_i \cos\psi_i)\ddot{\beta}_i + \sum^i \theta_F I_i \cos\psi_i \Omega^2\beta_i - \sum^i (h_v S_i \sin\psi_i)\ddot{\phi}_i \\
&- \sum^i h_v S_i \cos\psi_i\, 2\Omega\dot{\phi}_i + \sum^i h_v S_i \sin\psi_i \Omega^2\phi_i \quad = \quad h_v S_u \Omega^2 \cos\psi_1 + g[-h_v 2M_\beta \\
&+ \theta_F^2 S_u \cos\psi_1\, q_F - \theta_F\theta_L S_u \sin\psi_1\, q_L + \sum^i \theta_F S_i \beta_i] + Q_{FA}
\end{aligned} \tag{6}$$

$$\begin{aligned}
&- \theta_L[S_u \sin\psi_1 + \theta_F I_\beta \sin 2\psi_1]\ddot{q}_F + \theta_L\theta_F I_\beta(1 - \cos 2\psi_1)2\Omega\dot{q}_F + [M_{TL} + 2M_\beta \\
&+ \theta_L^2 I_\beta(1 - \cos 2\psi_1)]\ddot{q}_L + \theta_L^2 I_\beta \sin 2\psi_1\, 2\Omega\dot{q}_L + c_L\dot{q}_L + k_L q_L - \sum^i \theta_L I_i \sin\psi_i\ddot{\beta}_i \\
&- \sum^i \theta_L I_i \sin\psi_i \Omega^2\beta_i + \sum^i S_i \cos\psi_i\, \ddot{\phi}_i - \sum^i S_i \sin\psi_i\, 2\Omega\dot{\phi}_i - \sum^i S_i \cos\psi_i \Omega^2\phi_i \\
&= \quad S_u\Omega^2 \sin\psi_1 - g\theta_F\theta_L S_u \sin\psi_1 q_F + Q_{LA}
\end{aligned} \tag{7}$$

$$\begin{aligned}
&[S_i + \theta_F I_i \cos\psi_i]\ddot{q}_F - \theta_F I_i \sin\psi_i\, 2\Omega\dot{q}_F - \theta_L I_i \sin\psi_i\, \ddot{q}_L - \theta_L I_i \cos\psi_i\, 2\Omega\dot{q}_L \\
&+ I_i\ddot{\beta}_i + I_i\Omega^2\beta_i + c_\beta\dot{\beta}_i + k_\beta\beta_i \quad = \quad g[\theta_F S_i q_F + S_i \cos\psi_i\beta_i] + Q_{\beta_i A} \qquad i = 1,2
\end{aligned} \tag{8}$$

$$\begin{aligned}
&- h_v S_i \sin\psi_i\ddot{q}_F + S_i \cos\psi_i\ddot{q}_L + I_i\ddot{\phi}_i + c_\phi\dot{\phi}_i + k_\phi\phi_i \quad = \quad g[S_i \sin\psi_i \\
&+ S_i \cos\psi_i\phi_i] + Q_{\phi_i A} \qquad i = 1,2
\end{aligned} \tag{9}$$

n the above equations, the $k_n q_n$ and $c_n\dot{q}_n$ terms represent structural stiffness nd damping, the g terms represent the effect of gravity loads, and the Q_{nA} erms represent the aerodynamic forces. The M_{TF} and M_{TL} are the generalized ower masses corresponding to q_F and q_L respectively.

Some of the gravity loads act as stiffness terms in the equations. The blade coordinates $\psi_1 = \Omega t$ and $\psi_2 = \psi_1 + \pi$. For the two-bladed case, it is sometimes convenient to introduce the symmetric and antisymmetric blade variables,

$$\beta_s = (\beta_1 + \beta_2)/2, \qquad \beta_A = (\beta_1 - \beta_2)/2, \qquad \phi_s, \phi_A = \text{etc.} \tag{10}$$

to lessen the coupling between the degrees of freedom. Indeed, for a completely balanced rotor without gravity effects, the ϕ_s would be uncoupled from the other equations. In general though, all six coordinates are involved.

Equations (6) to (9) are a linear set of equations with periodic coefficients, subjected to gravity, rotor unbalance S_u, and aerodynamic wind forcing functions. The gravity loads act directly on the blades while the unbalance loads shake the tower which in turn couples into the blades. In addition to forced response, the homogeneous equations themselves may have strong instabilities present. These are generally investigated by the use of Floquet theory for these periodic coefficient equations. It should also be mentioned that for a three or more bladed rotor, the analysis is generally easier since one can eliminate the periodic coefficients by a suitable transformation of coordinates (at least for the balanced rotor, without gravity effects). See for example reference 7.

Various investigators have examined different subcases of equations (6) to (9). Coleman and Feingold (ref. 8) first looked at the case $q_F = 0$, $\beta_i = 0$, $\theta_L = 0$, with no gravity, unbalance, or aerodynamics present. Strong mechanical instabilities of a whirling nature were found to be possible at certain rotational speeds, involving coupling of lateral motion q_L with lag angle ϕ_A. This is the so-called "ground resonance" helicopter phenomenon. Reed (ref. 9) looked at the case $\beta_i = 0$, $\phi_i = 0$ with aerodynamics present. Again, strong instabilities were found involving q_L and the vertical $h_y q_F$ coupling through the mechanical and aerodynamic gyroscopic forces ($\Omega\dot{q}_F$, $\Omega\dot{q}_L$ terms). This is the so-called "propellor whirl" flutter. Young and Lytwyn (ref. 10) looked at the case $\phi_i = 0$ with aerodynamics present. This is essentially "propeller whirl" with flapping. Johnson (ref. 11) has looked in detail at the whole coupled system, but without gravity and unbalance effects in connection with his studies of proprotors. Equations very similar to the ones here are presented there. Finally, it should be mentioned there is a whole series of detailed investigations of rotors attached to fixed hubs ($q_F = 0$, $q_L = 0$) which emphasize the aerodynamic interaction between blade flapping, lagging, pitching and nonlinear dynamic effects brought on by large initial coning angles for the blades. See for example, references 4, 5, and 6.

EXPERIMENT

Some preliminary tests were run on a small .915 m (3.0 ft) diameter windmill placed in a wind tunnel. The general layout is shown in figure 2. The windmill had generally 2 blades, cantilevered in both the flap and lag directions. The approximately uniform, untwisted blades had a .0762 m(3 in) chord, and could be set at any incidence angle. For a few runs, 4 blades were attached to the windmill.

The weight of a typical blade was .175 kg (.386 lbs). The cantilever natural frequencies of the non-rotating blades were measured as 33, 93, 172, and 310 Hz for the 1st flap bending, 1st lag bending, 2nd flap bending, and 1st torsion modes respectively. These were corrected for rotational effects in the standard manner, $\omega_R^2 = \omega_{NR}^2 + L\Omega^2$, to give the rotating natural frequencies shown in figure 3. The tower stand had natural frequencies of 8.8, 16, 25 and 75 Hz for the lateral yawing, vertical pitching, lateral translation and vertical translation modes respectively. The windmill was instrumented to measure flap and lag bending moments at the blade root, and also lateral and vertical accelerations of the tower near the front bearing.

The wind tunnel was run to about 18 m/sec (59.1 ft/sec), and after taking data on windmill performance, the wind was turned off and the windmill would coast down to zero rotational speed. This gave a continuous frequency record through all the resonances of the system. Figures 4, 5, and 6 show the measured bending moments and accelerations from such sweeps for a blade setting angle $\theta = 0°$. Many superharmonic resonances can be seen for the flap and lag bending moments. These occur near integer orders of the rotation frequency as can be seen from figure 3. Particularly strong vibrations occured at 2 per revolution for both flap and lag. Indeed, lag moments near 10 times the static gravity moments are present at 50 Hz. The corresponding accelerations show a strong lateral resonance near 24 Hz. In these tests there was a small static unbalance due to unequal blade weights. Subsequent tests with another set of blades having a greater unbalance showed the same vibration patterns, but with peak amplitudes increased more than double. Also, tests run with four blades on the rotor showed similar strong resonances at 2 per revolution. The strong resonances in figures 4 to 6 seem then to have been caused by the rotating unbalance of the blade exciting tower stand frequencies which in turn excite blade frequencies superharmonically. Further details of these tests can be found in reference 12.

CONCLUSIONS

A brief review of some of the dynamic problems associated with large rotating windmills has been given, together with some preliminary experimental results. The importance of flexible towers and their interaction with the rotating blade dynamics has been discussed. Although much work has already been done in this area, many interesting dynamic problems remain to be resolved, particularly those involving rotors with built-in coning angles where nonlinear dynamics must be considered.

REFERENCES

1. Den Hartog, J.P.: Mechanical Vibrations. McGraw-Hill, New York, 4th Ed., 1956.

2. Loewy, R.G.: Review of Rotary-Wing V/STOL Dynamic and Aeroelastic Problems. J. of Amer. Helicopter Soc., Vol. 14, July 1969, pp. 3-24.

3. Rotorcraft Dynamic, NASA Special Publication, NASA SP-352, 1974.

4. Ormiston, R.A.: Rotor Dynamic Considerations for Large Wind Power Generator Systmes. Wind Energy Conversion Systems Workshop Proceedings, National Science Foundation NSF/RA/W-73-006, Dec. 1973.

5. Friedman, P.P.: Aeroelastic Modeling of Large Wind Turbines. Preprint No. S-990, 31st Annual National Forum of Amer. Helicopter Soc., Washington, D.C., May 1975.

6. Kaza, K.R.V.; and Hammond, C.E.: An Investigation of Flap-Lag Stability of Wind Turbine Rotors in the Presence of Velocity Gradients and Helicopter Rotors in Forward Flight. Proceedings of AIAA/ASME/SAE 17th Structures, Structural Dynamics, and Materials Conf., King of Prussia, Pennsylvania, May 5-7, 1976, pp. 421-431.

7. Hohenemser, K.H.; and Yin, S.K.: Some Applications of the Method of Multiblade Coordinates. J. of Amer. Helicopter Soc., Vol. 17, July 1972, pp. 3-12.

8. Coleman, R.P.; and Feingold, A.M.: Theory of Self-Excited Mechanical Oscillations of Helicopter Rotors with Hinged Blades. NACA Report 1351, 1958.

9. Reed, Wilmer H., III: Review of Propeller-Rotor Whirl Flutter. NASA Technical Report, TR R-264, July 1967.

10. Young, M.I.; and Lytwyn, R.T.: The Influence of Blade Flapping Restraint on the Dynamic Stability of Low Disk Loading Propeller-Rotors. J. of Amer. Helicopter Soc., Vol. 12, Oct. 1967, pp. 38-54.

11. Johnson, W.: Dynamics of Tilting Proprotor Aircraft in Cruise Flight. NASA Technical Note, TN D-7677, May 1974.

12. Miller, R.H.; et al: Wind Energy Conversion. Progress Report for Period July 15, 1975 - February 15, 1976 on NSF Grant No. AER 75-00826, RANN Document No. ERDA/NSF-00826/75-2, UC-60, Appendix III.

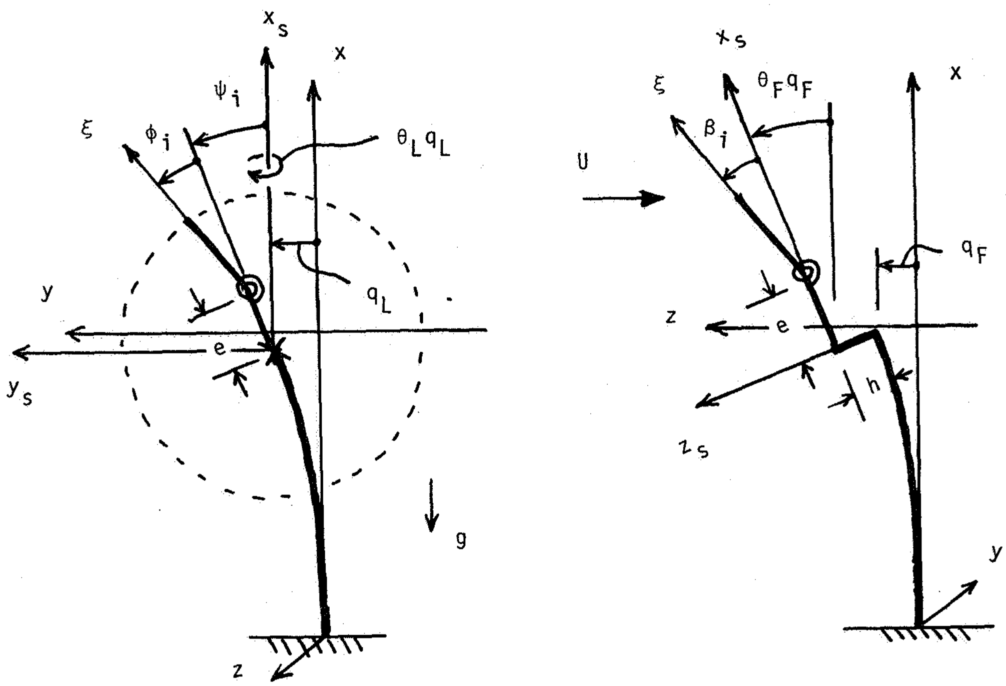

LOOKING DOWNSTREAM SIDE VIEW

Figure 1.- Analytic model for windmill-tower systems.

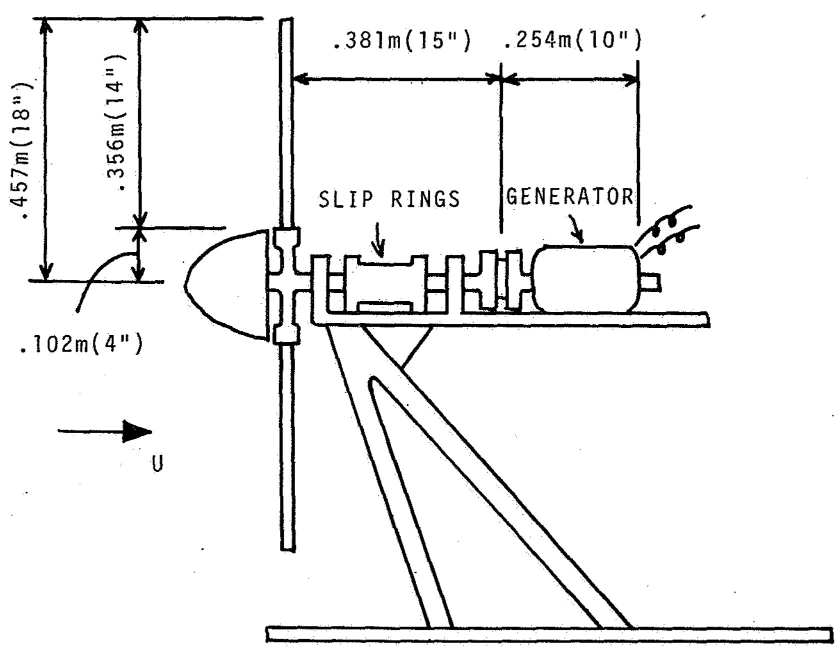

Figure 2.- Experimental layout of windmill assembly.

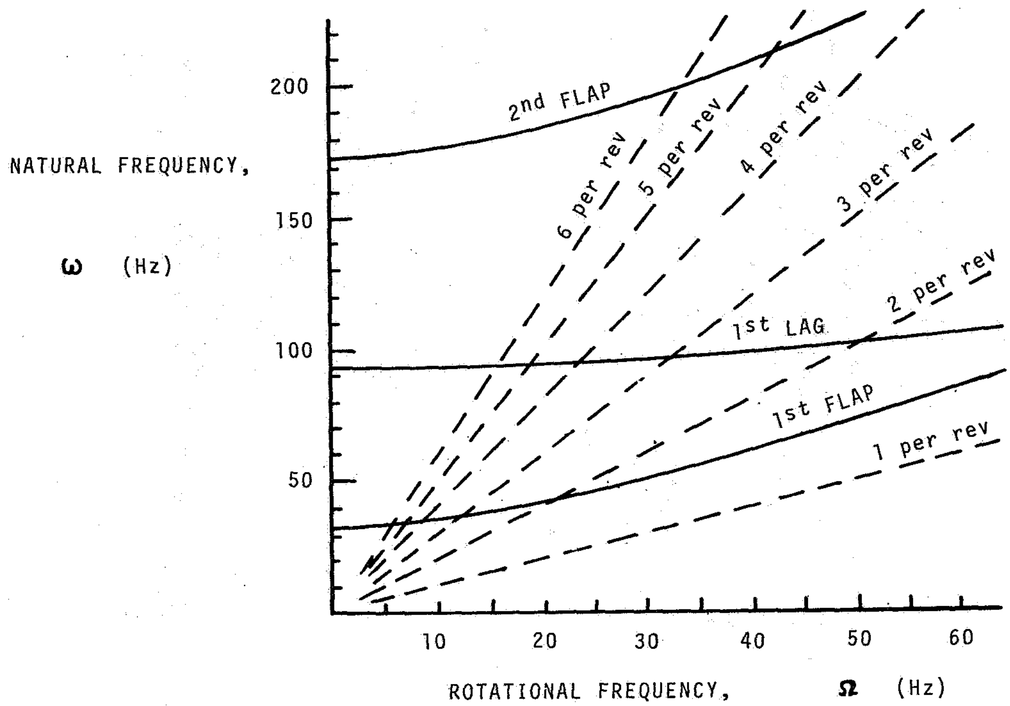

Figure 3.- Rotating natural frequencies of blades.

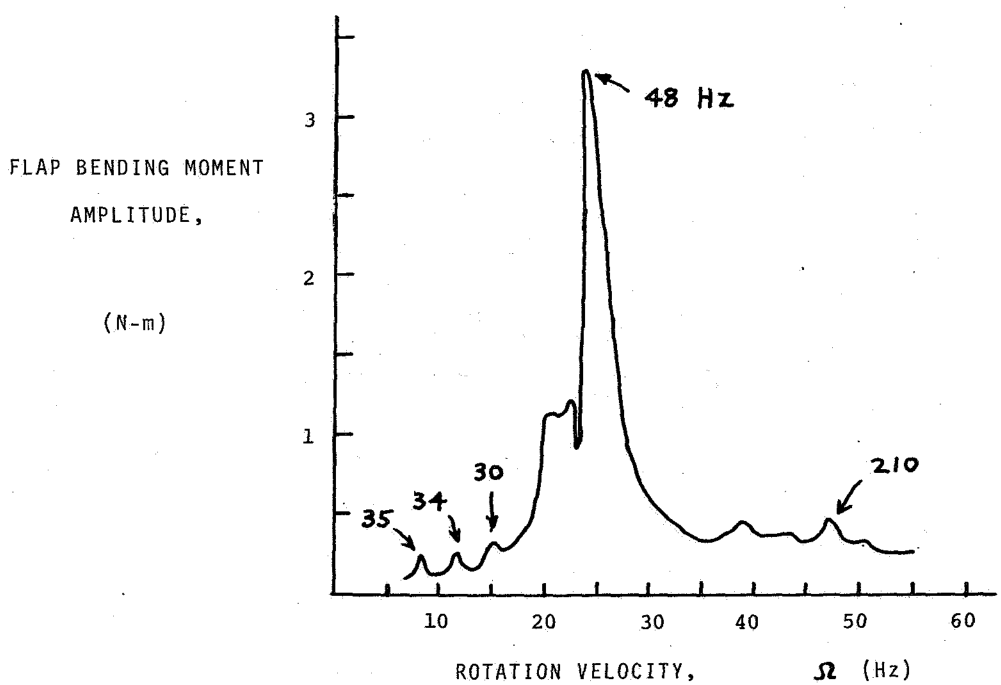

Figure 4.- Flap bending moment vibrations.

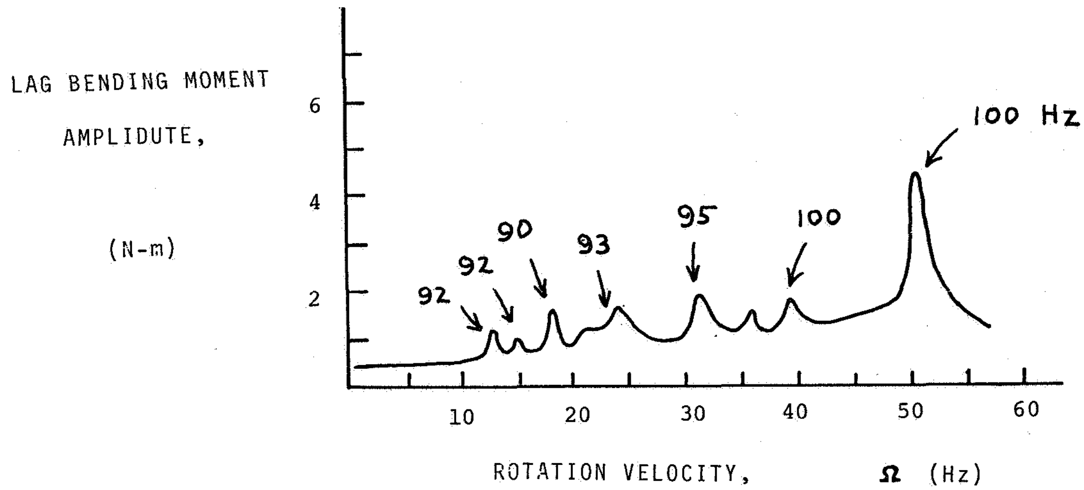

Figure 5.- Lag bending moment vibrations.

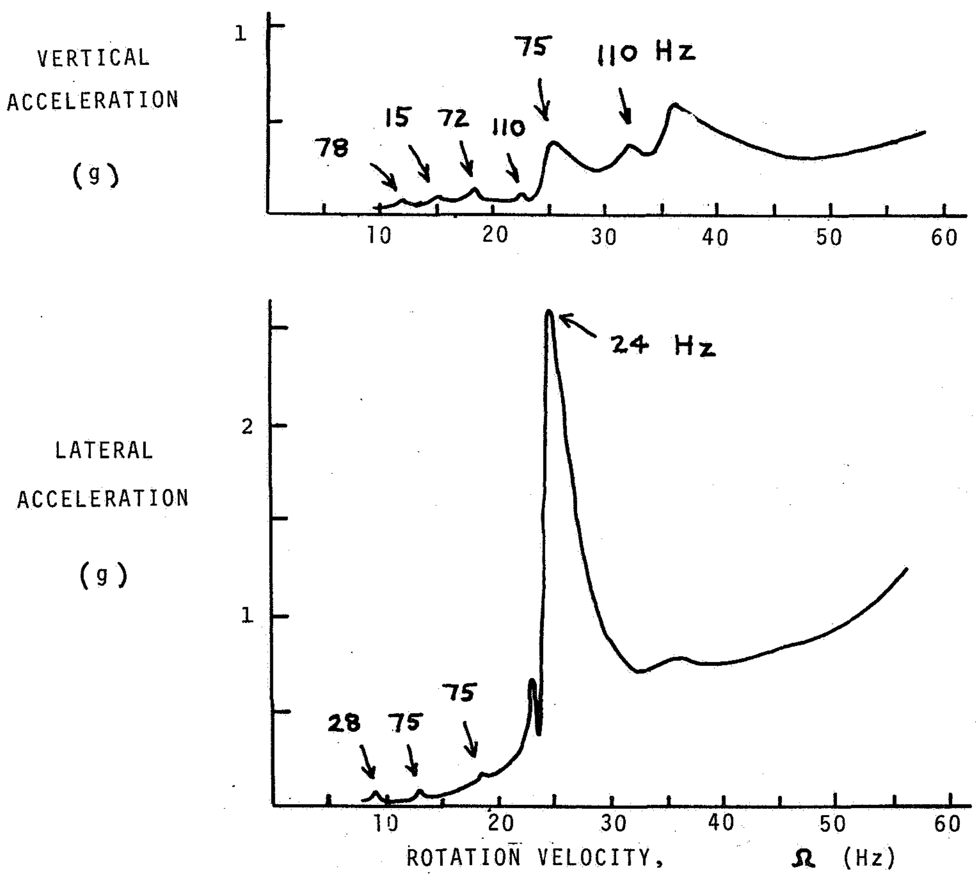

Figure 6.- Vertical and lateral tower accelerations.